Sensor and Simulation Notes

Note 384

November 1995

**Optimization of the Feed Impedance of Impulse Radiating Antennas
Part II: TEM Horns and Lens IRAs**

Everett G. Farr
Farr Research
614 Paseo Del Mar NE
Albuquerque, NM 87123

Abstract

In this note we continue the development of optimization problems for IRAs. Here we optimize the impedance for infinitely long TEM horns (an approximation for finite-length horns) and TEM horns with lenses, or lens IRAs. These calculations are analogous to those carried out for reflector IRAs in Part I of this paper [1]. We consider both TEM horns whose plates are flat, and whose plates are confined to a circular arc. We also consider configurations in which the fields in the entire aperture are allowed to radiate, and configurations in which only the fields between the plates are allowed to radiate.

I. Introduction

When designing TEM horns and lens IRAs for radiating a transient signal, it is unclear how best to choose the feed impedance to provide optimal performance. Normally, one has a fixed amount of aperture area within which to build the antenna, and one can choose any impedance one wants within this aperture. This paper addresses this problem for a number of configurations related to TEM horns and lens IRAs, as shown in Figure 1.1. We calculate here the feed impedances that produce the optimal radiation for a given input power, with the aperture constrained to a circle of a given radius.

This paper builds upon the work of [1], which treated the same problem with respect to reflector IRAs. The present problem is in some ways easier than the reflector IRA problem, since there is no need to consider aperture blockage due to the feed arms, as there was in [1].

We first treat the case of a TEM horn with flat, long plates, and with an infinite aperture. The plates are confined to a circular aperture of constant radius. Antenna gains are calculated as a function of impedance, and the feed impedances which achieve optimal gain are determined. This theory is then modified for the case where only the fields between the plates are allowed to radiate. This second case is useful in lens IRA design, in which only the fields between the plates are focused. Note that reflections from the dielectric lens are ignored, however, the error introduced by this effect is typically only a few percent. We then repeat the same calculations for a TEM horn built with curved plates, again treating the cases of an infinite aperture and a blocked aperture.

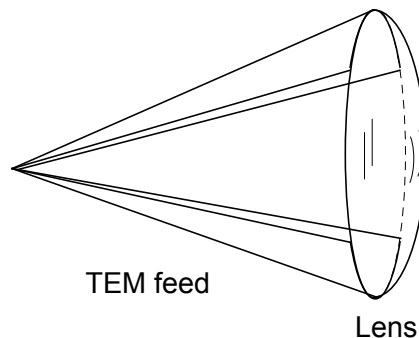Let us begin now with the case of a TEM horn built from flat plates.

Figure 1.1. A lens IRA, or without a lens, a TEM horn.

II. Optimization of a TEM horn with Flat Plates

The problem we wish to solve is shown in Figure 2.1. While keeping the flat plates within a circle of radius a_o, we determine how to choose b/a in such a way that optimizes the radiated field, for a given input power. This configuration is essentially what one would see if one looked at the front of a long TEM horn.

There are actually two problems that will be addressed. First, we assume an infinite aperture, as shown on the left in Figure 2.2. This is an approximation to a long TEM horn with no lens. Second, we consider the case where only the aperture fields between the plates are allowed to radiate. This would apply to a lens IRA, in which only a portion of the aperture is focused. It would also apply to an antenna that must be located behind a conducting wall.
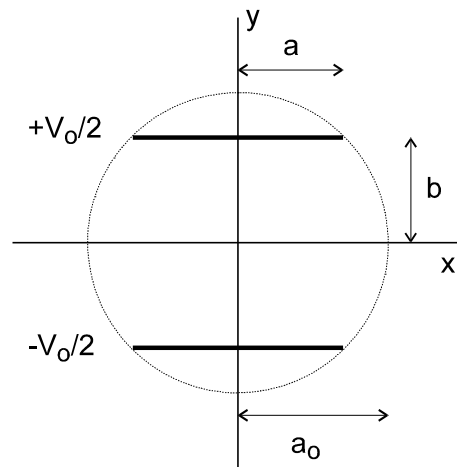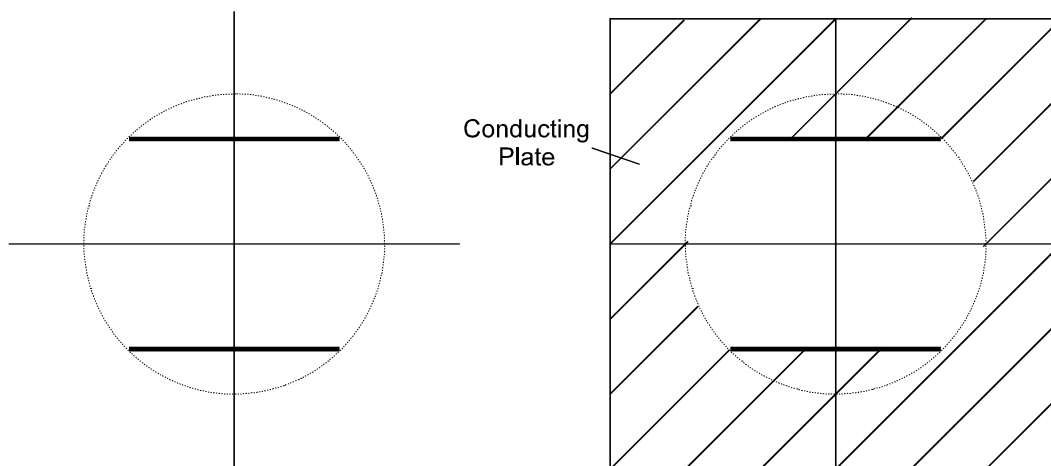

Figure 2.1. Configuration to be optimized.

Figure 2.2. Two cases for optimizing the radiated field of a flat TEM horn, infinite aperture (left) and blocked aperture (right).

First, we specify the characteristic impedance of the feed. The impedance is determined from [2,3]

$$f_g = \frac{K(m_1)}{K(m)} , \qquad m_1 = 1 - m$$

$$\frac{a}{b} = \frac{2}{\pi}\left[K(m)E(\phi_o|m) - E(m) F(\phi_o|m)\right] \qquad (2.1)$$

$$\sin(\phi_o) = \sqrt{\frac{1}{m}\left(1 - \frac{E(m)}{K(m)}\right)}$$

where $K(m)$ and $E(m)$ are the complete elliptic integrals of the first and second kind, and $F(\phi_o|m)$ and $E(\phi_o|m)$ are the incomplete elliptic integrals of the first and second kind. As usual, $f_g = Z_c/Z_o$, where $Z_o = 376.727\ \Omega$. To find f_g for a given value of b/a, one must solve numerically the above set of equations. Since the aperture is constrained to be of radius a_o, the relationship between a and b is expressed as

$$\frac{a^2}{a_o{}^2} + \frac{b^2}{a_o{}^2} = 1$$

$$b = \frac{a_o}{\sqrt{1 + (a/b)^2}} , \qquad a = \frac{a_o}{\sqrt{1 + (b/a)^2}} \qquad (2.2)$$

To obtain the radiated fields, we must find the fields in the aperture. Thus, we need to find a potential function in the form

$$\zeta = x + jy$$
$$w(\zeta) = u(\zeta) + jv(\zeta) \qquad (2.3)$$
$$x, y, u, \text{ and } v \text{ are all real}$$

When cast into this form, the aperture field and feed impedance are [2, 3]

$$E_y(x, y) = -\frac{V_o}{\Delta u}\frac{\partial u(x, y)}{\partial y}$$

$$f_g = \frac{\Delta u}{\Delta v} \qquad (2.4)$$

where Δu is the change in u from one conductor to the other, and Δv is the change in v as one goes around one conductor. We now need a suitable complex mapping to fit the problem.

The potential function that describes the aperture is [2, eqn. 2.15]

4

$$\frac{\zeta}{b} = \frac{2j}{\pi}\left[K(m)\,E(w|m_1) + w\times(E(m) - K(m))\right] \tag{2.5}$$

This is the simplest form. Another form is used in [3,4], but it is less convenient because the conductors are located on surfaces of constant v instead of the more customary constant u. As a cautionary note, we point out that most numerical packages expect the first argument of the incomplete elliptic function, $E(w|m)$, to be in the form of an angle. Thus, the incomplete elliptic integral has to be cast into the form of $E(\text{am}(w|m)|m)$, where $\text{am}(w|m) = \arcsin(\text{sn}(w|m))$ is the Jacobian amplitude function. A plot of the resulting complex mapping appears in Figure 2.3.
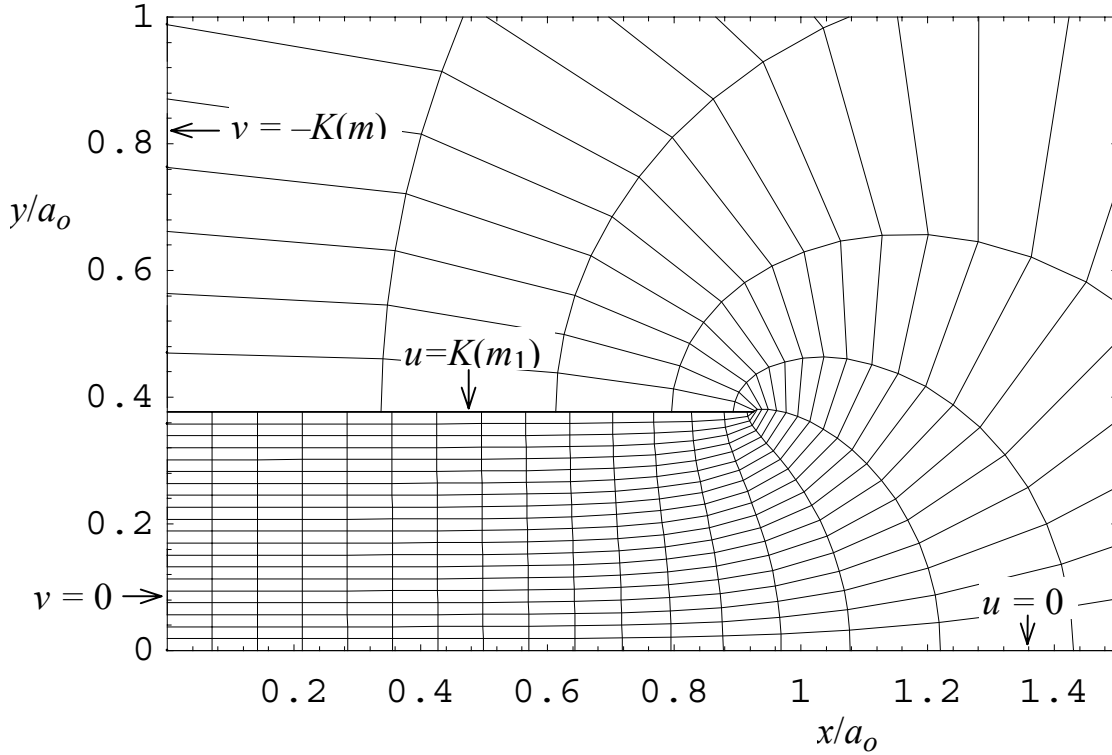

Figure 2.3. Complex potential map of the parallel plate configuration, for $Z_c = 100\ \Omega$

Next, the impedance was calculated using (2.1), and this is plotted as a function of b/a in Figure 2.4. Note that we have used a low-frequency asymptotic form of the impedance [3],

$$f_g = \frac{b/a}{1 + \dfrac{b/a}{\pi}\left[1 + \ln\left(\dfrac{2\pi}{b/a}\right)\right]} \tag{2.6}$$

This form was used for $b/a < 0.3$.

The figure of merit we use for the radiated field is the transient power gain (normalized to constant input power), as defined in [1,5,6]. Thus, we have

$$G_p = \frac{h_a}{\sqrt{f_g}} \tag{2.7}$$

where h_a is the normalized integral over the aperture field [7],

$$h_a = -\frac{f_g}{V_o} \iint_{S_a} E_y(x', y')\, dx'\, dy' \tag{2.8}$$

and S_a is the total surface over which radiation occurs. This integral will be calculated for the two configurations as a function of Z_c.

Let us pause for a moment, to consider whether the figure of merit, G_p, makes sense. To see why our expression of gain in (2.7) is reasonable, we recall that the fast part of the field radiated from an aperture on boresight is [6]

$$E_{rad}(t) = -\frac{h_a}{2\pi r c f_g}\frac{dV(t)}{dt}$$

$$E_{rad}(t) = -\frac{G_p}{2\pi r c}\frac{d\left(V(t)/\sqrt{f_g}\right)}{dt} \tag{2.9}$$

Furthermore, the received voltage for an incident field on boresight is

$$V_{rec}(t) = -h_a\, E_{inc}(t)$$

$$\frac{V_{rec}(t)}{\sqrt{f_g}} = -G_p\, E_{inc}(t) \tag{2.10}$$

Thus, both the radiated field and the received voltage are proportional to power gain. Note also that the voltage is cast into the form of square root of power, by dividing by $\sqrt{f_g}$. On this basis, our definition seems reasonable.
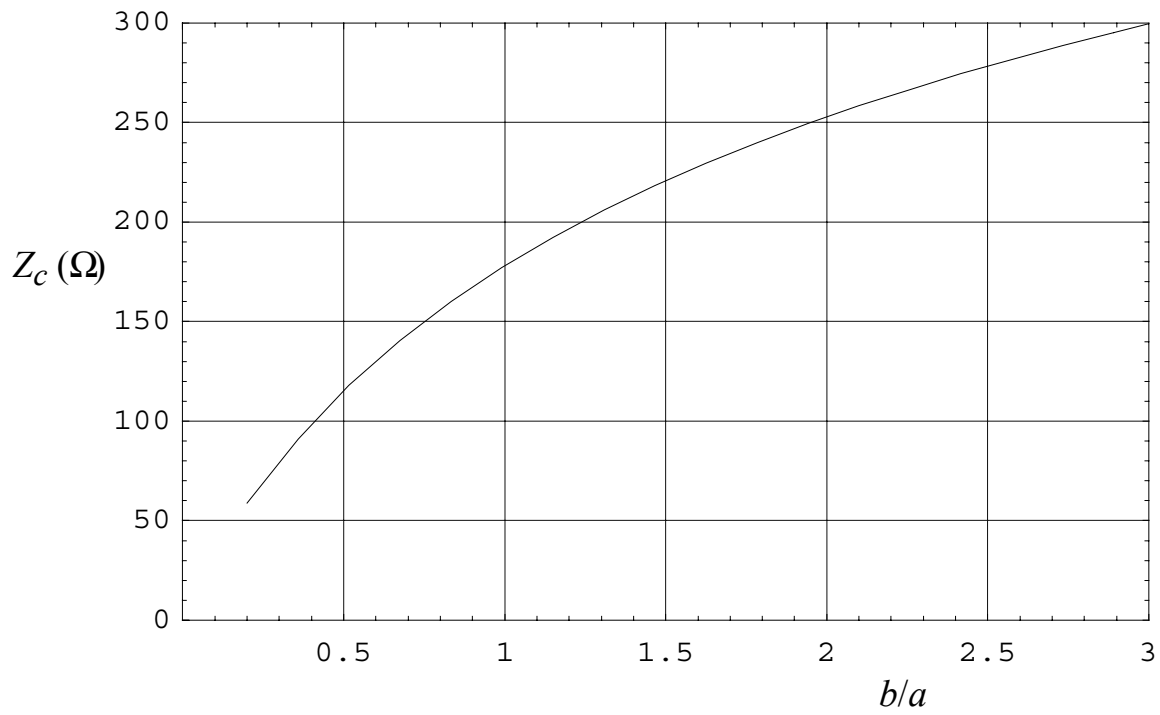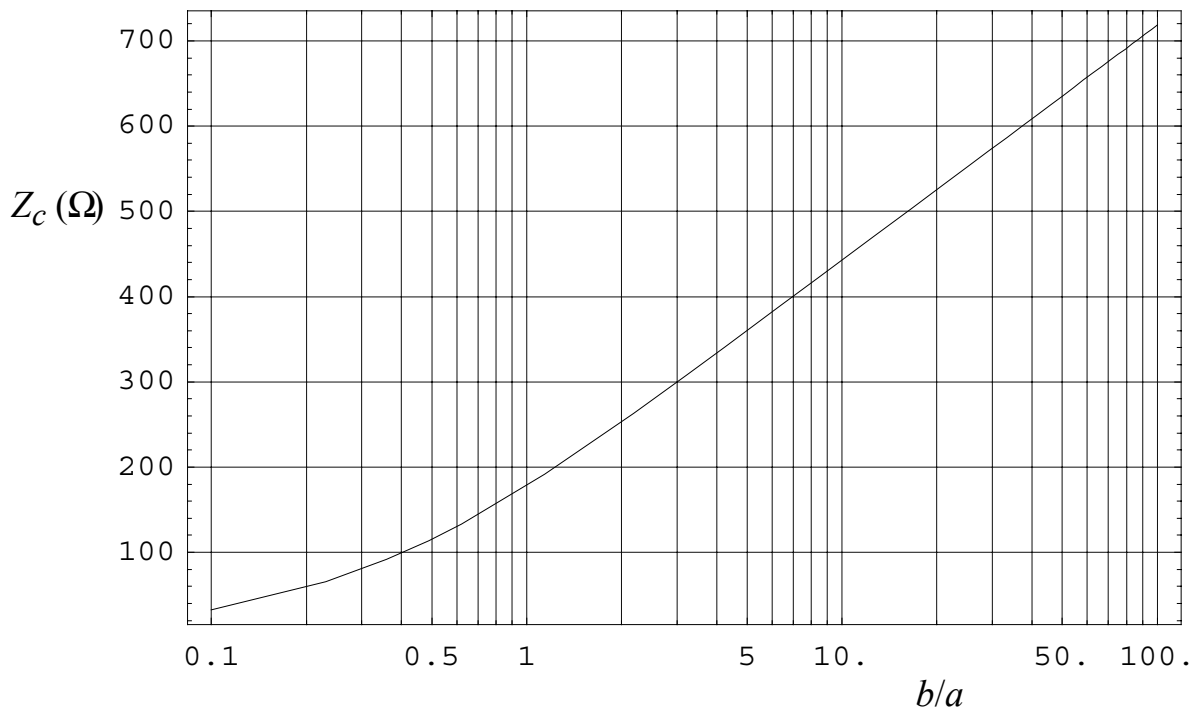
6

Figure 2.4. Impedance of two parallel plates.

A. Flat Plates with Infinite Aperture

We now calculate h_a and G_p for two cases. First, we consider the case of an infinite aperture, as shown on the left in Figure 2.2. In this case, it is particularly simple to calculate h_a, since it can alternatively be expressed in terms of the dipole moment of the charge in the aperture [7]. Thus,

$$h_a = \frac{\iint q(x, y)\, y\, dA}{\iint q(x, y)\, dA} \tag{2.11}$$

where $q(x, y)$ is the charge density on the conductors, and the integrals are carried out over all the conductors in the aperture. Since all the charge is located at $y = \pm b$, the value of h_a is calculated trivially as

$$h_a = b \tag{2.12}$$

We have plotted h_a/a_o as a function of Z_c in Figure 2.5. As expected, at high impedances it approaches unity asymptotically. This is the expected result because for a pair of thin wires, we know from [7] that $h_a = a_o$.

Finally, we have plotted the power gain, $G_p = h_a / \sqrt{f_g}$, in Figure 2.6. The peak occurs at $Z_c = 242.3\ \Omega$, where the power gain is $1.09 \times a_o$. At this point, $b/a = 1.82$.
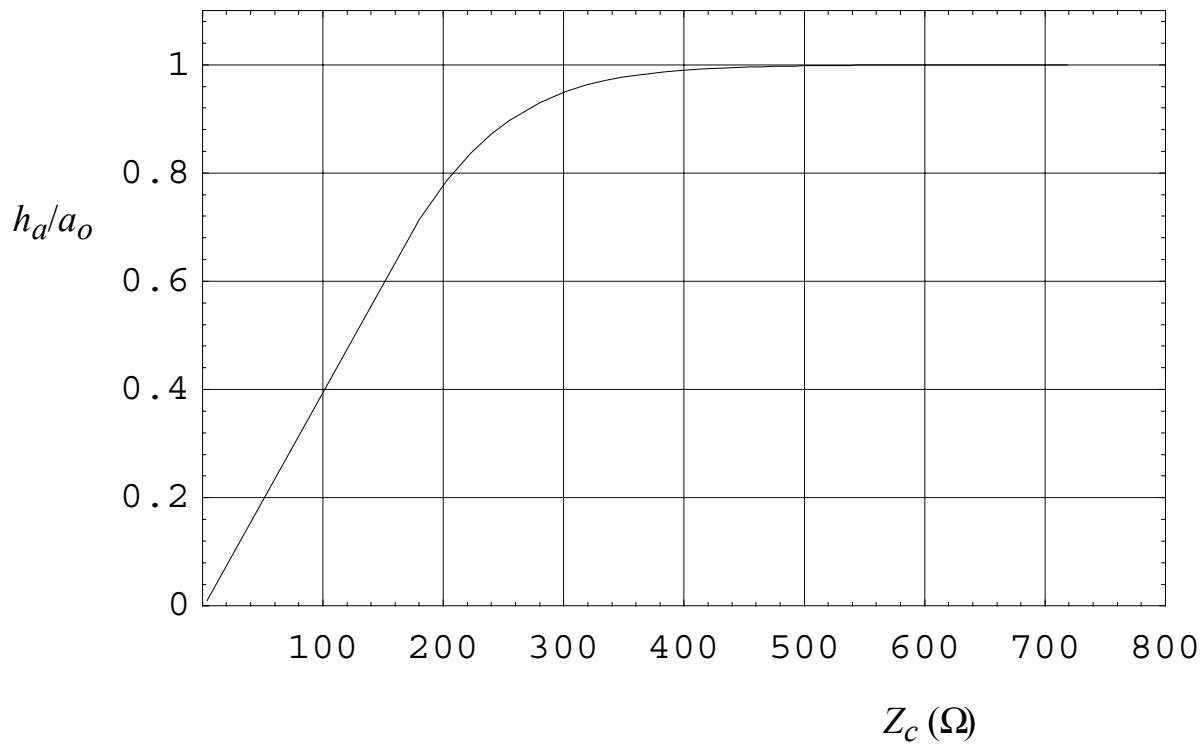
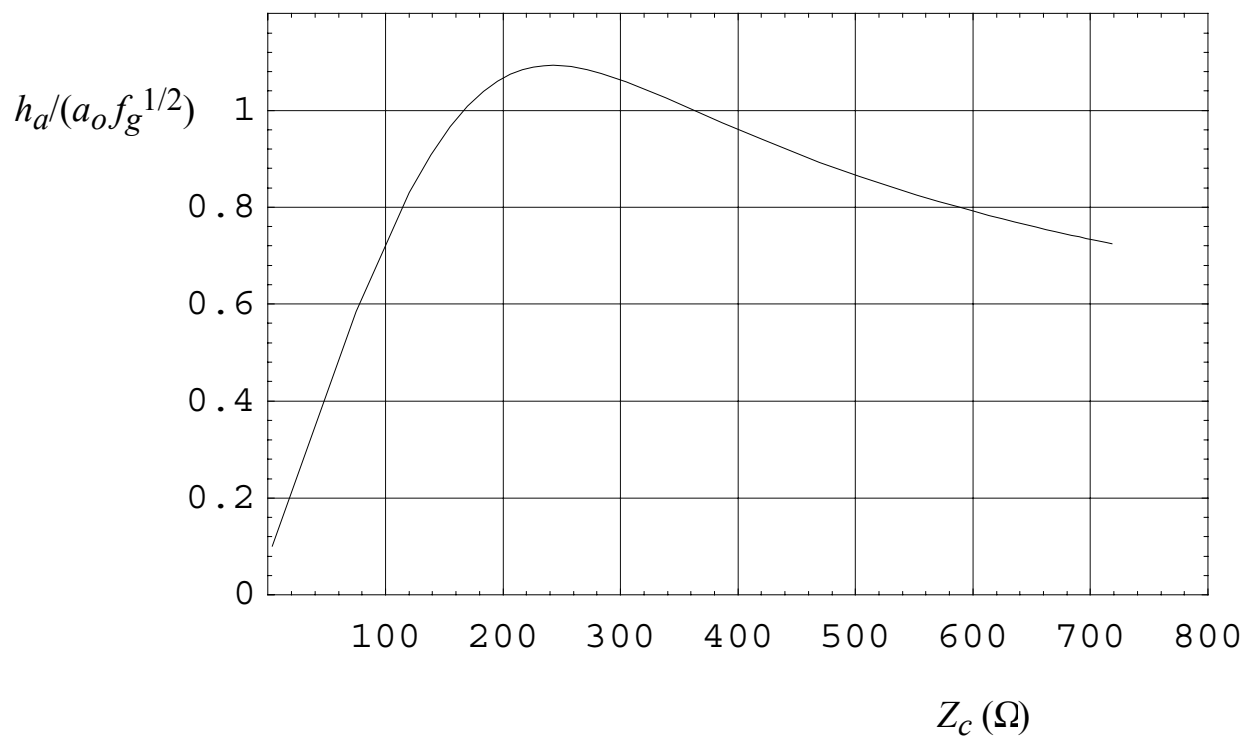Figure 2.5. Normalized aperture height for the infinite aperture with flat plates.

Figure 2.6. Normalized power gain for the infinite aperture with flat plates.

9

B. Flat Plates with Blocked Aperture

Next, we calculate h_a for the case of a blocked aperture, as shown on the right in Figure 2.2. This is the normal case of interest to the antenna designer. Only a portion of the aperture field is included in the aperture integral, because only that portion is focused.

To calculate h_a, we express it as a contour integral [1,6,7], i.e.,

$$h_a = -\frac{4}{\Delta v} \oint_{C_a} v(\zeta)\, dy \qquad (2.13)$$

where Δv is the change in v around a conductor. In addition, C_a is a contour integral over one quadrant of the exposed portion of the aperture, as shown in Figure 2.7. To calculate this integral, we note that the integrals over C_1 and C_3 are identically 0, since there is no change in y. Furthermore, the integral over C_4 is also zero, because $v = 0$ there. Therefore, we need only calculate the integral over C_2.
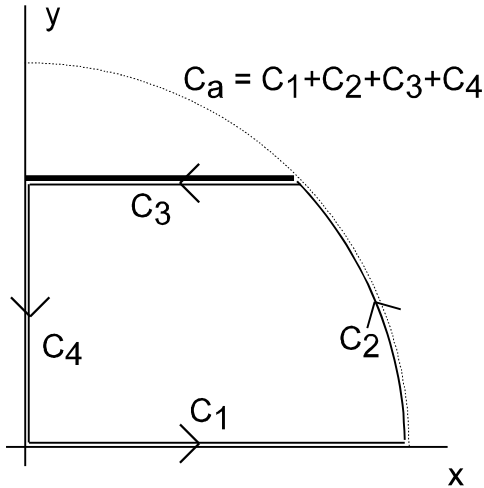

Figure 2.7. Definition of the contour C_a.

Calculating the integral over C_2 presents us with a challenge, because there is no easy way to calculate $v(\zeta)$. Normally, one would find v from the complex contour mapping, i.e., equation (2.5). But in the present case there is no simple way to invert the contour mapping to find v in terms of ζ. Thus, one would have to solve (2.5) numerically for $v(\zeta)$ at each location on the arc. Since we must also calculate the integral along this path, this becomes computationally expensive.

A simpler method is to just assume that the contour C_2 is along a contour of constant v. This is rigorously true in the limit of high impedances, $b/a \rightarrow \infty$, because the conductors

become thin wires at that point. Since we know the optimal values will occur at relatively high values of b/a, the approximation is reasonable. Thus, we search numerically for the value of v that intersects the circle at $(x, y) = (a_o, 0)$, and use that for our contour of constant v_o. From (2.5), we solve numerically the following for v_o,

$$\frac{a_o}{b} \;=\; \frac{2\,j}{\pi}\left[K(m)\,E(j\,v_o|m_1) \;+\; j\,v_o\times(E(m)-K(m))\right] \tag{2.14}$$

After finding v_o, and using the fact that $\Delta v = 2K(m)$, we find the aperture height to be

$$h_a \;=\; -\frac{2\,b\,v_o}{K(m)} \tag{2.15}$$

Note that v_o is a negative number, so h_a is positive, as it must be. We estimate the error in this procedure to be a few percent. A catalog of contour maps (like those of Figure 2.3) with various values of b/a is available in [8]. From these contour maps, one can verify our estimate of the accuracy of the method.

The results for h_a are plotted in Figure 2.8, and the power gain is plotted in Figure 2.9. The peak gain occurs at $Z_c = 203.7\ \Omega$, where the power gain is $1.16 \times a_o$. At this point, $b/a = 1.28$.

At this point we can check the validity of our numerical approximations. In particular, we check the validity of our assumption that the edge of the circular aperture is approximated by a line of constant v. A plot of the contour map for the optimal value of $b/a = 1.28$ is shown in Figure 2.10. Also plotted on the map is the circular arc that defines the aperture. Based on this plot, the error estimate of a few percent seems reasonable. Note also that our estimates of h_a and G_p are lower than their actual values, so we are slightly underestimating the true power gain of this configuration.

It is interesting to compare the results for the blocked aperture to those with the infinite aperture. One might expect that an infinitely large aperture would have better performance, but that is not the case. The blocked aperture actually has a slightly better power gain, with a value of $1.16 \times a_o$, compared to $1.09 \times a_o$ for the infinite aperture. The likely reason for this is that we have blocked out fields that have a negative contribution to the total radiated field, just above the top plate and just below the bottom plate. Therefore, if one wanted to improve the performance of a simple long TEM horn, one would block out a portion of the field just above and below the top and bottom plates.
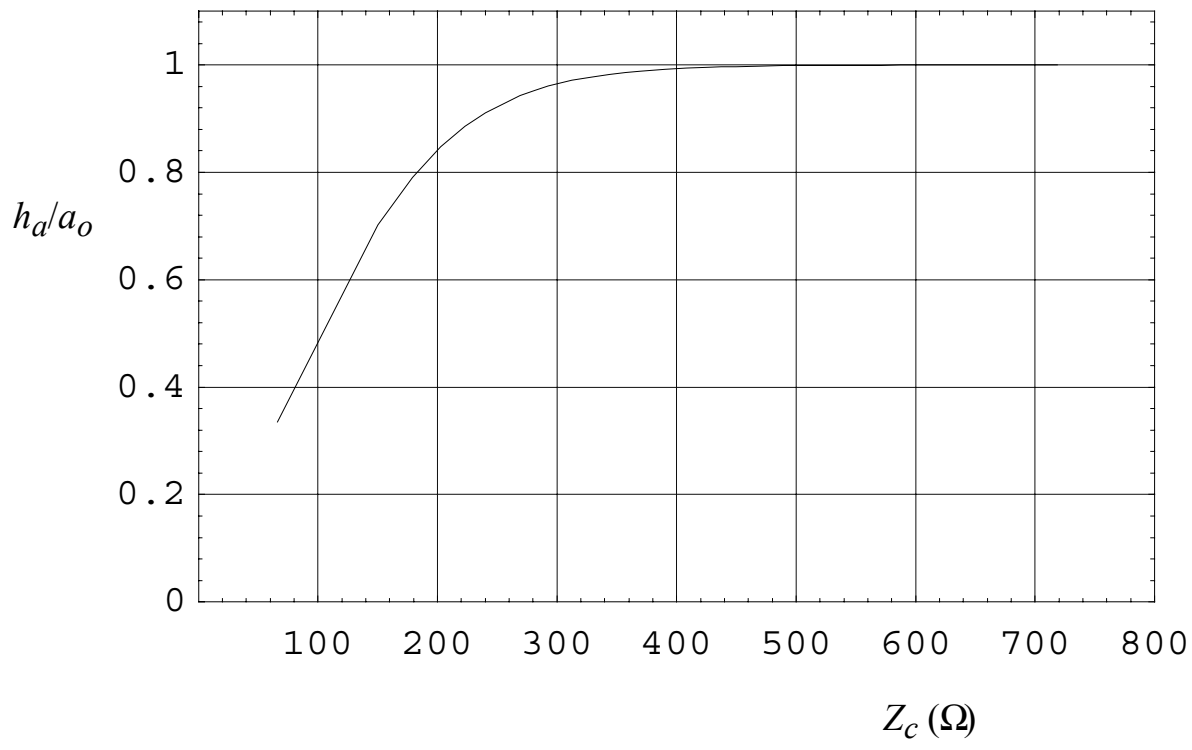
Figure 2.8. Normalized aperture height for the blocked aperture with flat plates.
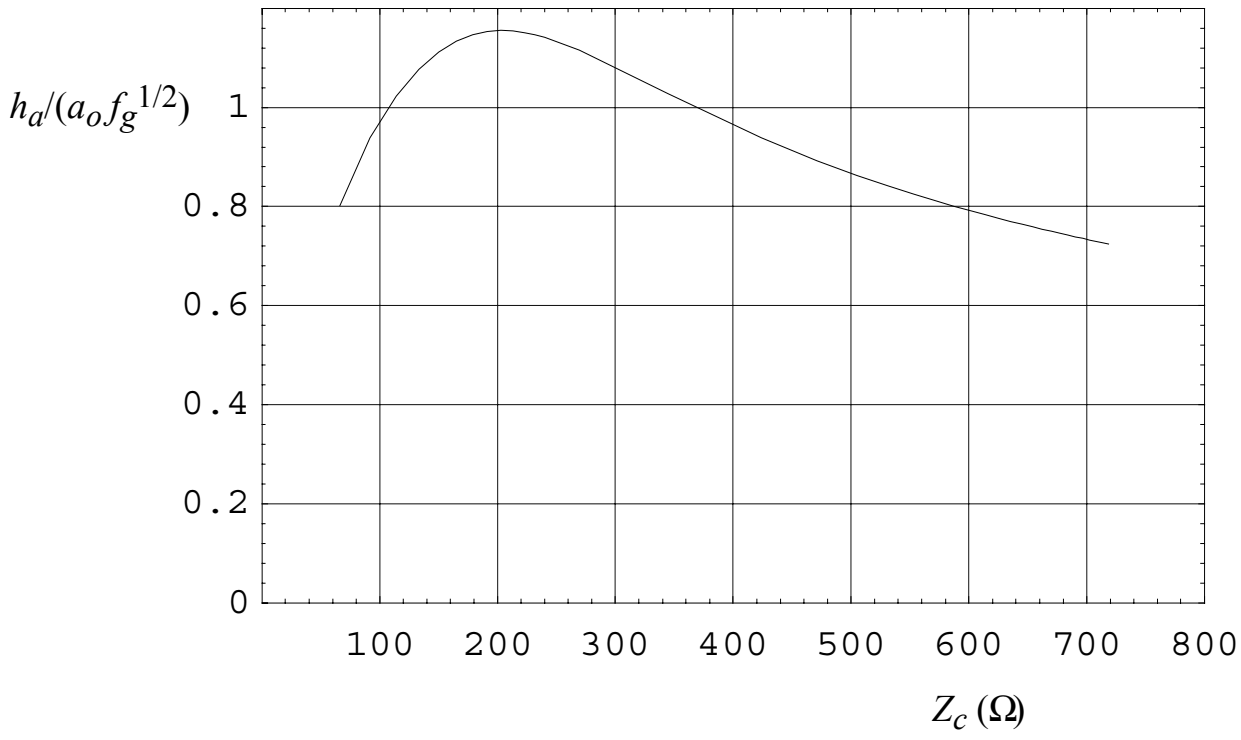

Figure 2.9. Normalized power gain for the blocked aperture with flat plates.
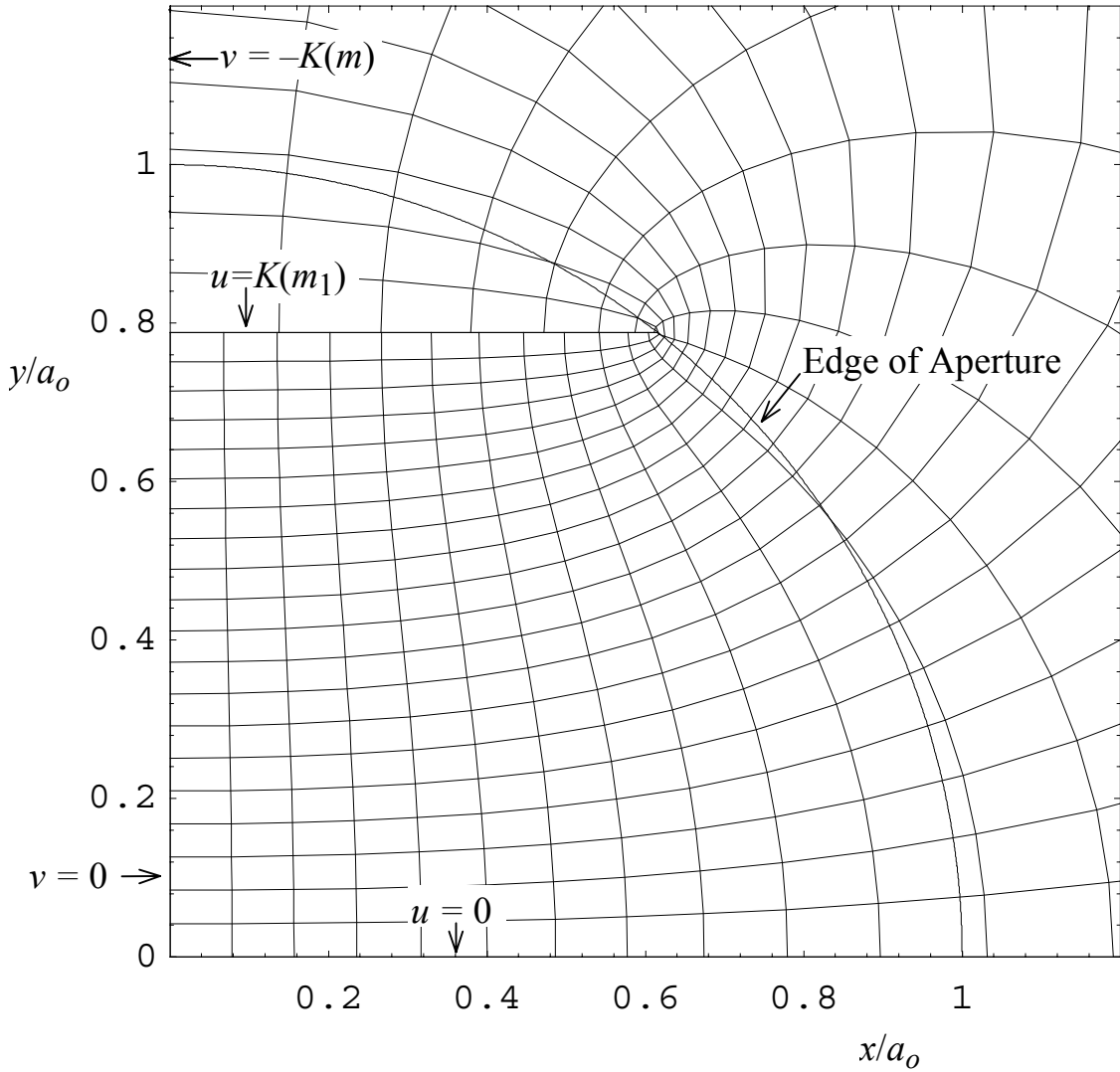
Figure 2.10. Contour map for the optimal configuration with blocked aperture of $b/a = 1.28$, and $Z_c = 203.7 \ \Omega$. Note that the v contour near the edge of the aperture is approximately the same as the circle, thus validating the theory used to calculate h_a and G_p.

III. Optimization of a TEM horn with Curved Plates

We now repeat the calculations of the previous section using curved plates, instead of flat plates. The configuration is shown in Figure 3.1. To solve this problem, we now must determine the optimal angle α for the plates. Once again, both the infinite aperture and the blocked aperture will be considered, as shown in Figure 3.2.

As before, we first establish the characteristic impedance and the aperture field. The characteristic impedance of the configuration is $Z_c = Z_o f_g$, where [9]
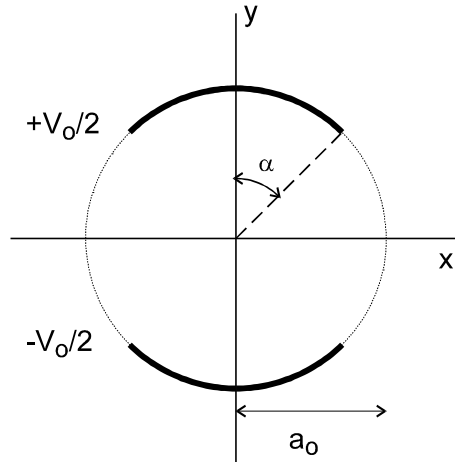

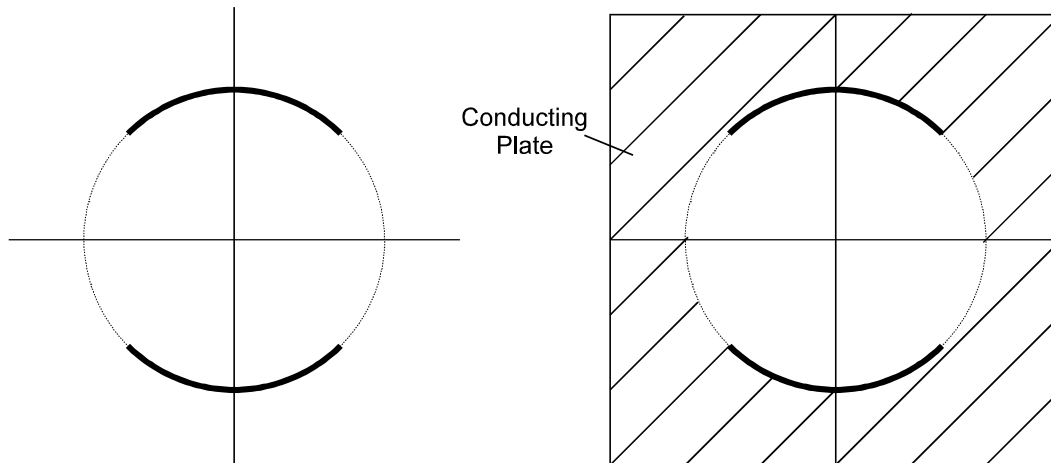Figure 3.1. Configuration to be optimized.

Figure 3.2. Two cases for optimizing the radiated field, infinite aperture (left) and blocked aperture (right).

14

$$f_g = \frac{K(m)}{K(m_1)} \quad , \qquad m_1 = 1 - m \tag{3.1}$$

and

$$m = \left[\frac{1-\sin(\alpha)}{\cos(\alpha)}\right]^4 \quad , \qquad \tan(\alpha) = \frac{1-m^{\frac{1}{2}}}{2\,m^{\frac{1}{4}}} \tag{3.2}$$

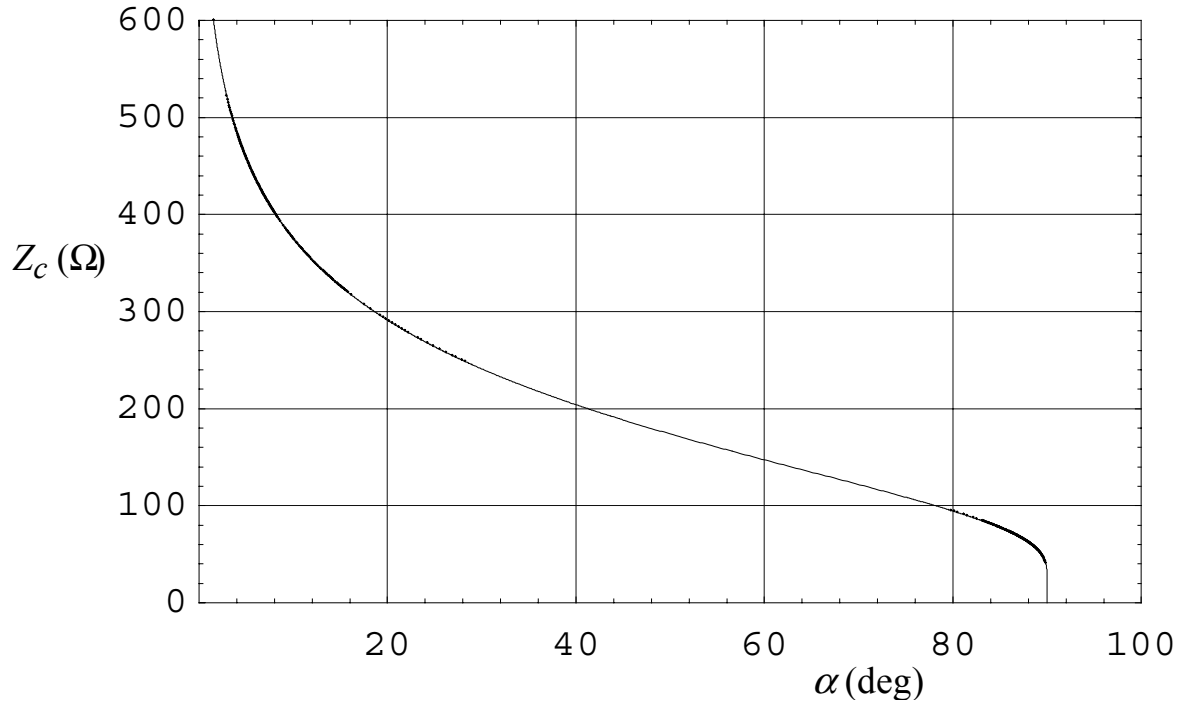We have plotted Z_c as a function of α in Figure 3.3.

Figure 3.3. Impedance of curved plates as a function of α

The potential function describing this configuration is [9]

$$w = \text{arcsn}\left[\frac{1}{j\,m^{\frac{1}{4}}}\frac{(\zeta/a_o)-1}{(\zeta/a_o)+1}\right] \quad , \qquad \frac{\zeta}{a_o} = \frac{1+j\,m^{\frac{1}{4}}\text{sn}(w|m)}{1-j\,m^{\frac{1}{4}}\text{sn}(w|m)} \tag{3.3}$$

where $\text{sn}(w|m)$ is one of the Jacobian elliptic functions [10], and arcsn is its inverse. This complex potential is plotted in Figure 3.4.

With these preliminaries established, we now calculate for our two cases the values of h_a and G_p, as already defined in (2.7) and (2.8).
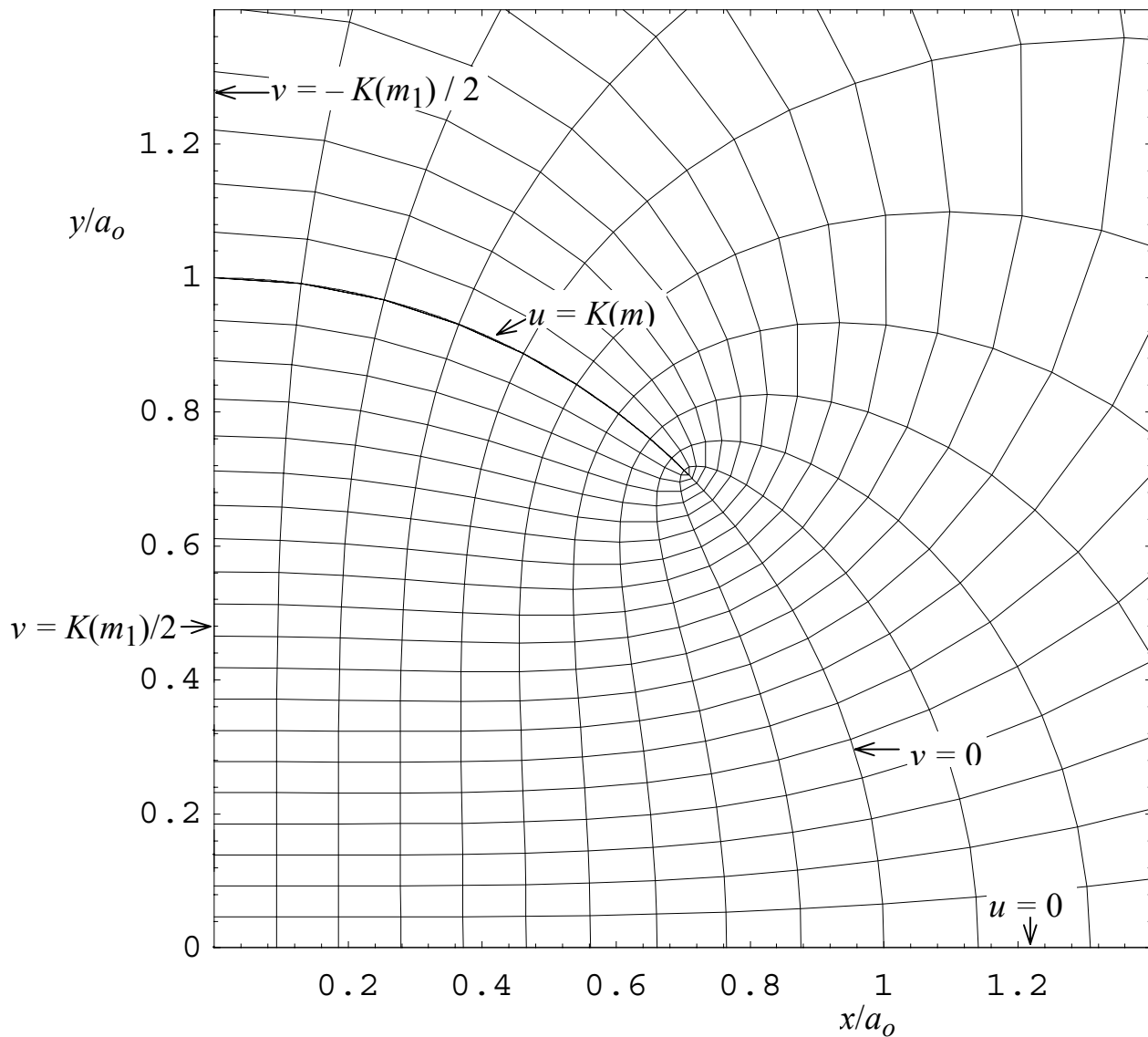
Figure 3.4. Complex potential map for a circular TEM horn.

A. Curved Plates with Blocked Aperture

Of the two cases we treat in this section, the simplest is when the aperture is blocked, as shown on the right in Figure 3.2. In this case, one can use the circular aperture theory of [11] to find h_a. It was shown there that the step-response radiated field on boresight due to any analytic field contained within a circular aperture is simply

$$E(r,t) = E_o \frac{a_o{}^2}{2cr} \delta_a(t) \tag{3.4}$$

16

where E_o is the field at the center of a circular aperture of radius a_o, and $\delta_a(t)$ is an approximation to the delta function [7]. On the other hand, the radiated field can also be expressed as

$$E(r,t) \; = \; -\frac{V_o}{r}\,\frac{h_a}{2\pi c\,f_g}\,\delta_a(t) \tag{3.5}$$

Combining the above two equations leads to

$$h_a \; = \; -\frac{\pi\,a_o{}^2\,f_g\,E_o}{V_o} \tag{3.6}$$

For the current configuration, the electric field at the center of the aperture is [9]

$$E_o \; = \; -\frac{V_o}{a_o}\,\frac{1}{K(m)(1+m^{1/2})} \tag{3.7}$$

Combining the above two equations, and using (3.1) for f_g, the aperture height is just

$$h_a \; = \; -\frac{\pi\,a_o}{K(m_1)(1+m^{1/2})} \tag{3.8}$$

Note that as $m \to 1$, the plate width becomes very small. Furthermore, $K(m_1) \to \pi/2$ and $h_a \to a_o$, as we know it must.

One might question the validity of the circular aperture theory used here, because of the singularity in the fields at the edge of the curved plates. Recall that one of the requirements imposed on the solution in [11] is that there must be no field singularities in the aperture, since a singularity cannot be represented by a Fourier expansion of circular harmonics. But our singularity occurs at the edge of the aperture, and one can take a boundary around the aperture that is some ε inside the previous boundary. In doing so, one can eliminate the singularity, and in the limit as $\varepsilon \to 0$, the aperture integral is the same as it would have been with no singularity on the edge. Thus, the circular aperture theory of [11] is valid for our configuration.

Although it is not really necessary, we note that there are other ways of calculating the effective aperture height. In particular, one can calculate h_a as a contour integral as before, as [1,7]

$$h_a \; = \; -\frac{4}{\Delta v}\,\oint_{C_a} v(\zeta)\,dy \tag{3.9}$$

where C_a is the contour shown in Figure 3.5. To calculate this integral, we note that the integral over C_1 is 0, since there is no change in y. The integral over C_2 also zero, because $v = 0$ there.

Finally, the integral over C_4 is trivial because it is along a contour of constant $v = K(m_1)/2$. Thus, the integral over C_4 is just

$$\oint_{C_4} v(\zeta)\,dy \;=\; -\frac{a_o\,K(m_1)}{2} \tag{3.10}$$

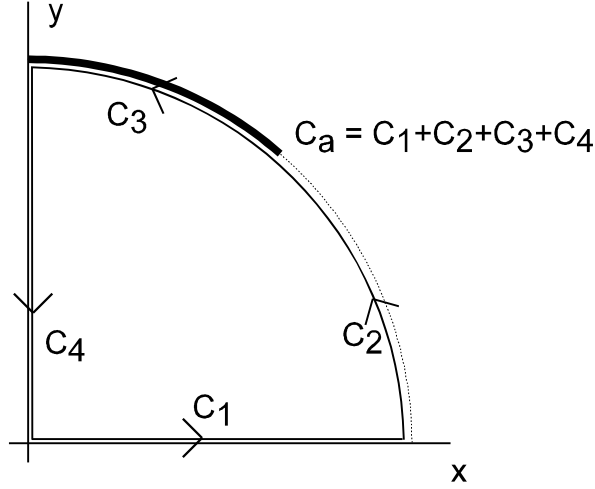This leaves us with just the integral over C_3 to calculate.

Figure 3.5. Definition of the contour C_a.

The challenging part of the contour integral is along C_3. It turns out that we can calculate this numerically, by integrating along a path where $\zeta = a_o\,e^{j\theta}$, calculating $v(\zeta)$ as the imaginary part of $w(\zeta)$ as expressed in (3.3). Using the fact that $y = a_o \sin(\theta)$ and $dy = a_o \cos(\theta)\,d\theta$, we have

$$\oint_{C_3} v(\zeta)\,dy \;=\; a_o \int_{\pi/2-\alpha}^{\pi/2} \mathrm{Im}[w(e^{j\theta})]\cos(\theta)\,d\theta \tag{3.11}$$

Combining the above three equations, and noting that $\Delta v = 2\,K(m_1)$, we find

$$h_a \;=\; a_o \left[1 \;-\; \frac{2}{K(m_1)} \int_{\pi/2-\alpha}^{\pi/2} \mathrm{Im}[w(e^{j\theta})]\cos(\theta)\,d\theta \right] \tag{3.12}$$

There is no need to actually use the above formula in the optimization procedure, since we can use (3.8) much more efficiently. Nevertheless, we have compared the numerical results obtained with the two methods, and they are in agreement to machine precision.

18

We have calculated h_a as a function of impedance in Figure 3.6. Furthermore, the power gain G_p , as defined earlier in (2.7), is shown in Figure 3.7. The peak occurs at $Z_c = 376.727/2$ Ω ($f_g = 0.5$), where the power gain is $1.20 \times a_o$. At this point, $\alpha = 45^o$. Thus, there is a pleasing symmetry in the result.
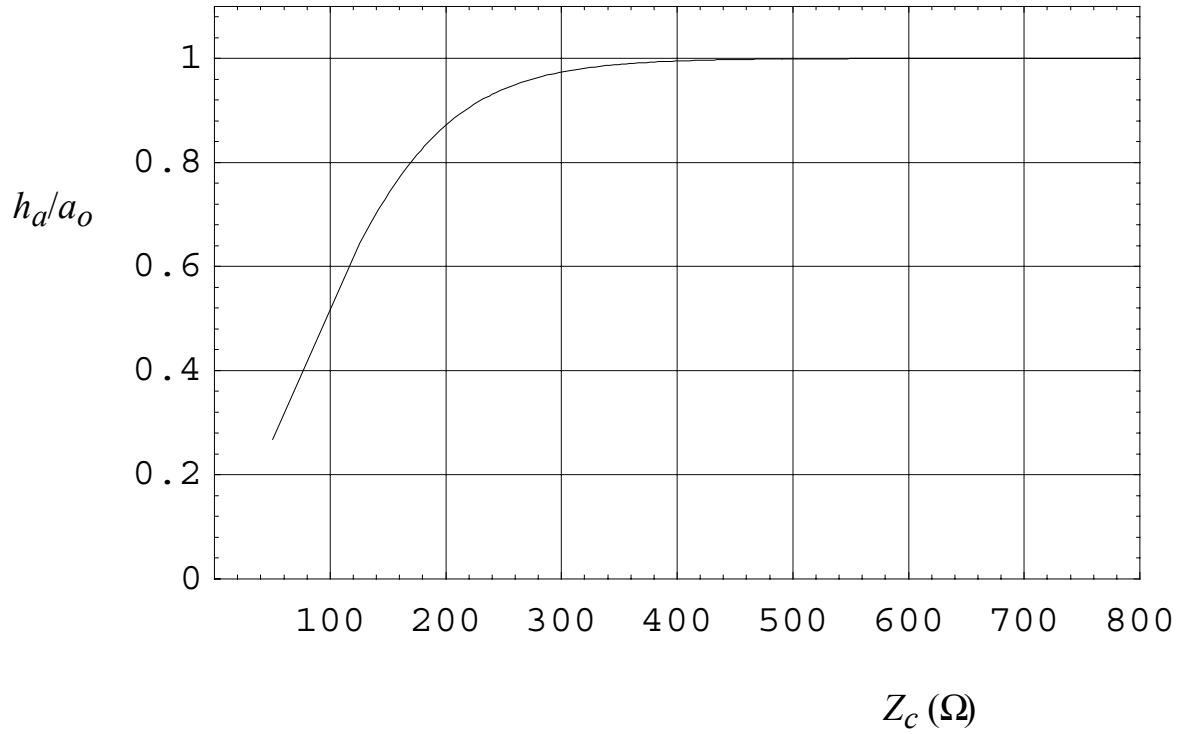
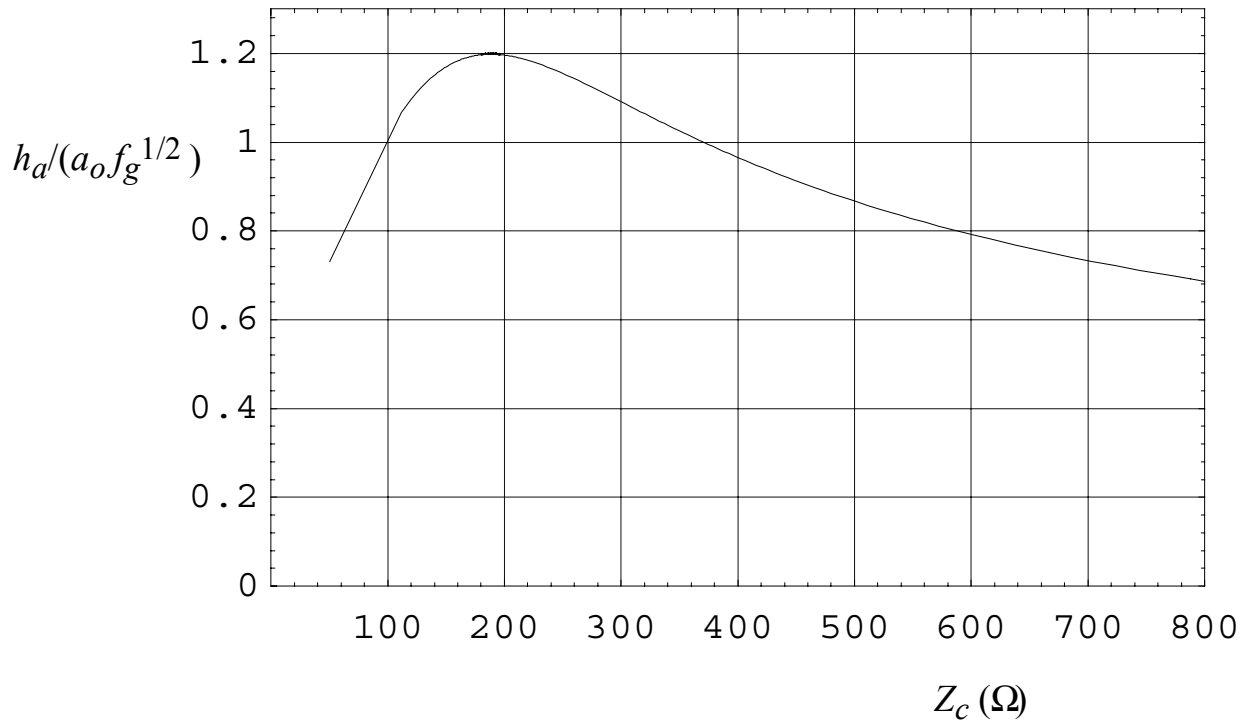Figure 3.6. Normalized aperture height for the blocked aperture with curved plates.

Figure 3.7. Normalized power gain for the blocked aperture with curved plates.

B. Curved Plates with Infinite Aperture

Finally, we consider curved plates with an infinite aperture, or with the conducting plate removed, as shown on the left in Figure 3.2. It turns out that for this particular configuration, the results with the blocked aperture are exactly the same as those for the infinite aperture, so there are no additional calculations to perform. Thus, we find once again that the peak gain of $1.20 \times a_o$ occurs at $f_g = 0.5$, where $\alpha = 45^o$

The reasoning for this result has to do with the properties of self-reciprocal apertures, as developed in [12]. Briefly, it was shown there that when an infinite aperture has the property that it is self reciprocal, the radiated field on boresight is described by the field at the center of the aperture (equation 3.4), exactly as for circular apertures [11]. Since we just used [11] to find the result for a blocked aperture, there is no need to repeat the calculation. .

As a check on this result, we can calculate h_a using the electric dipole moment technique in (2.11). The charge on the plates is proportional to the difference in electric fields just above and below the plates. Thus, we modify the formula slightly to express this, i.e.,

$$h_a = \frac{\int |E(\zeta_+) - E(\zeta_-)| \, y \, d\theta}{\int |E(\zeta_+) - E(\zeta_-)| \, d\theta} \qquad (3.13)$$

where the integral is taken over the plates. Note also that $E(\zeta_+)$ and $E(\zeta_-)$ are the electric fields just above and below the plates, and that these fields are in the radial direction, because they must be normal to the conductor. The electric field is expressed as [9]

$$E(\zeta) = E_x - j E_y = \frac{j V_o}{a_o K(m)(1 + \sqrt{m})} \frac{1}{\sqrt{(\zeta / a_o)^4 + 2\cos(2\alpha)(\zeta / a_o)^2 + 1}} \qquad (3.14)$$

where $\zeta_{\pm} = a_o(1 \pm \varepsilon) e^{j\theta}$ just above and below the plates, and ε is a vanishingly small number. We have carried out this calculation numerically, and we have found the results for h_a (and hence G_p) to be the same as those calculated earlier to within machine precision.

It is interesting to compare this result to an earlier paper [9], which calculated optimal field uniformity for the same configuration. It was found in [9] that maximum field uniformity at the center of the aperture also occurs at $f_g = 0.5$ and $\alpha = 45^o$. Since it is believed that maximum field uniformity leads to maximum radiated field, our result appears to be quite reasonable.

21

IV. Conclusions

We have found the optimal impedances for long TEM horns and lens IRAs, for the cases of blocked apertures and infinite apertures, when the antennas are confined to remain within a circle of a given radius. The optimal results are summarized in Table 4.1. As perhaps we might have expected, either of the two configurations with curved plates has the highest gain, since they more completely fill the available aperture. However, the flat-plate configuration with blocked aperture is not far behind.

Table 4.1 Summary of Optimal Configurations

Configuration	Figure of Merit G_p / a_o	Z_c (Ω)	Relevant Parameter
Circular Plates, Blocked or Infinite Aperture	1.20	188.4	$\alpha = 45^o$
Flat Plates, Blocked Aperture	1.16	203.7	$b/a = 1.28$
Flat Plates, Infinite Aperture	1.09	242.3	$b/a = 1.82$

References

1. E. G. Farr, Optimizing the Feed Impedance of Impulse Radiating Antennas, Part I, Reflector IRAs, Sensor and Simulation Note 354, January 1993.

2. C. E. Baum, D. V. Giri, and R. D. Gonzalez, Electromagnetic Field Distribution of the TEM Mode in a Symmetrical Two-Parallel-Plate Transmission Line, Sensor and Simulation Note 219, April 1976.

3. C. E. Baum, Impedances and Field Distributions for Parallel Plate Transmission Line Simulators, Sensor and Simulation Note 21, June 1966.

4. P. Moon and D. E. Spencer, Field Theory Handbook, second edition, Springer-Verlag, Berlin, 1971.

5. E. G. Farr and C. E. Baum, Extending the Definitions of Antenna Gain and Radiation Pattern Into the Time Domain, Sensor and Simulation Note 350, November 1992.

6. E. G. Farr, C. E. Baum, and C. J. Buchenauer, Impulse Radiating Antennas, Part II, pp. 159-170 in *Ultra-Wideband, Short-Pulse Electromagnetics 2*, New York, Plenum Press, 1995.

7. C. E. Baum, Aperture Efficiencies for IRAs, Sensor and Simulation Note 328, June 1991.

8. T. L. Brown and K. D. Granzow, A Parameter Study of Two Parallel Plate Transmission Line Simulators of EMP Sensor and Simulation Note XXI, Sensor and Simulation Note 52, April 1968.

9. T. K. Liu, Impedances and Field Distributions of Curved Parallel-Plate Transmission-Line Simulators, Sensor and Simulation Note 170, February 1973.

10. M. Abramowitz and I. A. Stegun, *Handbook of Mathematical Functions*, National Bureau of Standards, June 1964.

11. C. E. Baum, Circular Aperture Antennas in Time Domain, Sensor and Simulation Note 351, November 1992.

12. E. G. Farr and C. E. Baum, Radiation from Self Reciprocal Apertures, Chapter 6 in C. E. Baum and H. N Kritikos (eds.), *Electromagnetic Symmetry*, Taylor and Francis, 1995, Section 6.5, pp. 300-304. Also appears as Sensor and Simulation Note 357 April 1993.